

# Investigation of the effect of mechanical activation on the structural changes of fluorapatite using X-ray diffraction analysis method

A Hadi Shadi Naghadeh<sup>1</sup>, Parviz Pourghahramani<sup>2\*</sup>

1. Ph. D. of Mineral Processing, Mining Investment, Insurance Company (MICO), Iran.

2\*. Professor of Mineral processing, Sahand University, Tabriz, Iran.

## Abstract

In this study, a planetary ball mill was used for mechanical activation of phosphate concentrate by dry milling in argon atmosphere. To investigate the structural changes of fluorapatite, amorphization degree, crystallite size, micro-strain, particles size, specific surface area changes and new phase formation were investigated. The crystallite size and micro-strain were estimated using Williamson-Hall method. To investigate the influence of effective parameters on mechanical activation, the ball to powder ratio of 20:1 and 40:1 with two types of balls of 9.4 and 20 mm and speeds of 200 and 500 rpm was used. The results showed that agglomeration of particles occur at higher intensities of mechanical activation, but no phase change occurs during high intensity ball milling. The most variations in crystallite size, micro-strain, surface area, amorphization degree and XRD line broadening were for samples that were activated by smaller balls for longer time. The results of the Williamson-Hall plots showed that the maximum effect of mechanical activation on phosphate concentrate was in the first 20 minutes with small balls and the crystallite size, micro-strain and amorphization degree was changed from 225 nm, 0.09% and 0% for initial sample to 64.29 nm, 0.9% and 80.081% for mechanically activated sample, respectively. Also the results showed that changes in cell parameter at c direction had larger effect on unit cell volume. The maximum unit cell volume variations were corresponding to mechanically activated sample with 9.4 mm balls that changed from 525.4 (Å<sup>3</sup>) for initial sample to 528 (Å<sup>3</sup>) for activated one after 90 min.

\*To whom correspondence should be addressed:  
pourghahramani@sut.ac.ir

*Journal of Advanced  
Environmental  
Research and  
Technology*

Vol. 1, No.2  
page 41-53, spring 2023  
\*\*\*

Received 12 November 2022  
Accepted 28 February 2023

## key words

phosphate concentrate  
fluorapatite  
mechanical activation  
microstructure  
planetary ball mill



## 1. Introduction

Mechanical activation is a branch of mechano-chemistry used to activate chemical reactions using mechanical energy. In the mineral processing, milling has different uses and is generally divided into three parts: coarse grinding, fine grinding, and mechanical activation. Unlike mechanical activation that is performed to make changes in structure, stress state, and reactivity of minerals, the main purpose of fine and coarse grinding is to reduce particle size. However, the particle size reduction occurs during mechanical activation as well [1].

In the mineral processing, mechanical activation is used to produce ultrafine particles with high specific surface area and chemical reactivity. Mechanical activation uses high intensity milling to change material properties to have a high surface area, dislocations and defects in crystal structure, polymorphic transformations, chemical reactions, decomposition, ion exchanges, and oxidation – reduction reactions and also cause solids to reach an activated state [2].

The development of researches has shown that mechanical activation increases the severity of structural defects and increases the material reactivity [3-5]. In the strain- stress curves, the fine grinding is limited to the transformation of brittle to ductile limit, but regardless of the initial size, the decrease in particle size during mechanical activation occurs as a result of a change in grinding regime from brittle to ductile. These changes are accompanied by a strain increase and thus cause dislocations in the particles. These dislocation cause an increase in structural distortions that influence the reactivity of the particles [5]. In the case of mechanical activation, the direct relationship between particle size reduction and milling intensity is unreliable [6].

Mechanical activation increases the free energy of particles by increasing the surface free energy and volumetric elastic strain energy. Thus, crushed particles with high intensity milling are activated and the gained free energy can be released with different energy transfer methods [7].

A great deal of research has been done to investigate the behavior of materials after mechanical activation [8-13]. The effect of mechanical activation on morphological changes of hematite has been investigated. The results showed that, the particles were crushed at lower levels of mechanical energy and by increasing of applied energy; particles were agglomerated, crystallite size decreased but, spe-

cific surface area, amorphization degree and micro-strain were increased [14]. Structural changes, particle size and specific surface area variations in mechanically activated hematite concentrate using different mills and in various operating conditions have been investigated. The results showed that, regardless of the type of used mill, by decreasing the size of the balls, the specific surface area of the activated particles and the broadening of the X-ray diffraction lines increased. The highest amount of X-ray diffraction amorphous phase was associated with planetary ball mill and the lowest was with tumbling mill. Calculating the energy contribution to structural defects showed that the highest portion of stored energy in mechanically activated hematite was related to the contribution of amorphization. In this regard, the planetary ball mill caused the highest amount of excess energy in activated particles [15, 16].

X-ray diffraction line profile analysis has been accepted as a non-destructive method for investigating the behavior of mechanically activated powders. X-ray diffraction profiles, which have been recorded from mechanically activated minerals, show broadening due to structural defects in crystallites. X-ray diffraction line broadening is generally due to crystallite size and micro-strain variation. Therefore, we can obtain useful information from the crystallite size, micro-strain variations and dislocations created during high intensity ball milling [16].

In this study, line profile analysis method was used to obtain information about the structure of mechanically activated phosphate concentrate in argon atmosphere. In most studies, mechanical activation of sulfide and pure materials has been studied. The purpose of this study was to investigate the effect of mechanical activation using a planetary ball mill on the structural changes of the fluorapatite in phosphate concentrate using the X-ray diffraction line profile analysis method, which has not been studied yet. The structural properties of the mechanically activated fluorapatite were investigated in a quantitative and qualitative manner as a function of activation time with using the Williamson-Hall integral breadth method.

## 2. Materials and method

### 2.1. sample preparation and characterization

The sample used in this study was prepared from Esfardi phosphate flotation plant concentrate located in Yazd province, 35 km northeast of Bafgh.

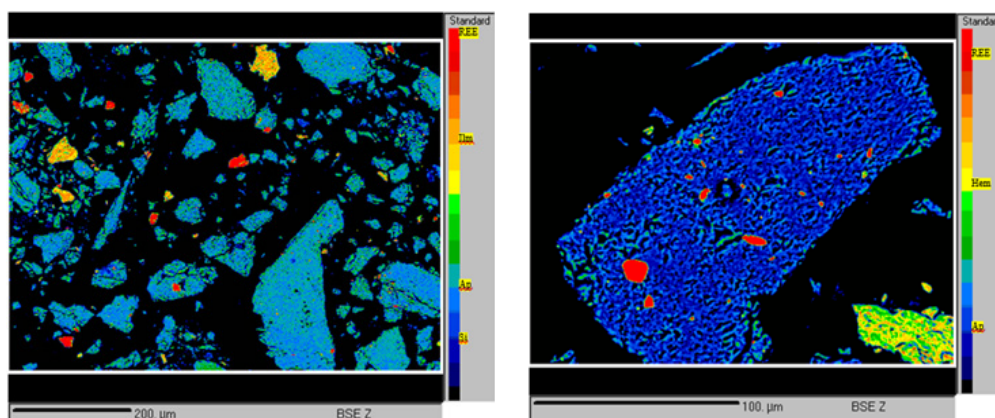


Figure 1: EMPA analysis results of Esfordi phosphate concentrate.

Using the standard method of the sample preparation, the representative sample was prepared for identification, mechanical activation, and leaching tests. The d80 of representative sample was 67 microns. Figure 1 shows EMPA analysis of phosphate concentrate. The main minerals of phosphate concentrate were fluorapatite, hematite, calcite, quartz rarely monazite, xenotime and ilmenite. The particle size of the rare earth minerals were between 1 and 20 microns, but in some cases they were up to 50 microns, which were usually liberated. In general, d80 of rare earth minerals (monazite and xenotime) were about 20 microns. As the figure 1 shows, rare earth minerals are often found in apatite (more than 90%), sometimes found within the

The XRD analysis of the phosphate concentrate and standard sample was performed by Bruker Axs D8 advanced instrument and the results are shown in Figures 2 and 1. In all experiments, Co K $\alpha$  beam of 1.791 Angstroms was used. The scanning counting time and step size was 5 seconds and 0.01 degrees, respectively, and the range of scanning angle were selected, according to the conditions of the specimens, in the range of 18 to 50 degrees. The standard sample (LaB6 SMR-660a) was used to eliminate the instrumental effect on the broadening of the XRD profiles. Fluorapatite, hematite, calcite, quartz and maghemite are the most abundant minerals in phosphate concentrates, respectively.

Table 1: chemical analysis of Esfordi phosphate concentrate

Rare earth elements	Ce	Nd	La	Y	Pr	Sm	Gd	Dy	Er	Eu	Lu	Tb	Yb
Assay (ppm)	5608	2228	1959	679.7	614.05	342.85	188.07	154.05	129.77	29.4	4.26	42.6	31.7
Main elements	Ca	P	Fe	F	Cl								
Assay (%)	37.13	16.31	2.91	3	0.3								

hematite or the border between apatite and quartz.

The ICP-MS analysis method was applied to elemental characterization of the sample, which results are shown in Table 1. Cerium (5608 ppm), Neodymium (2227 ppm), Lanthanum (1959 ppm), Yttrium (679 ppm) and Praseodymium (614 ppm) were the most important rare earth elements in the phosphate concentrate. These five elements account for about 92% of the total rare earth element concentrate. Ce, Nd and La elements account for 82% of all the rare earth elements in the sample. Therefore, Esfordi phosphate concentrate is a light rare earth element concentrate and contains about 1.2% of rare earth elements, totally.

## 2.2. Mechanical activation

A planetary ball mill (Pulverisette 6, FRITSCH, Germany) was used to mechanically activate of phosphate concentrate. The balls used for mechanical activation were of steel type with a diameter of 9.4 and 20 mm. For investigating of mechanical activation effects on the phosphate concentrate structure, ball to powder ratio of 20:1 and 40:1 at milling times of 20, 60 and 90 min and revolution speeds of 200 and 500 rpm was used. Milling tests were performed under argon atmosphere to prevent possible chemical reactions. For each 20-minute period milling, 20 minutes of rest were considered.

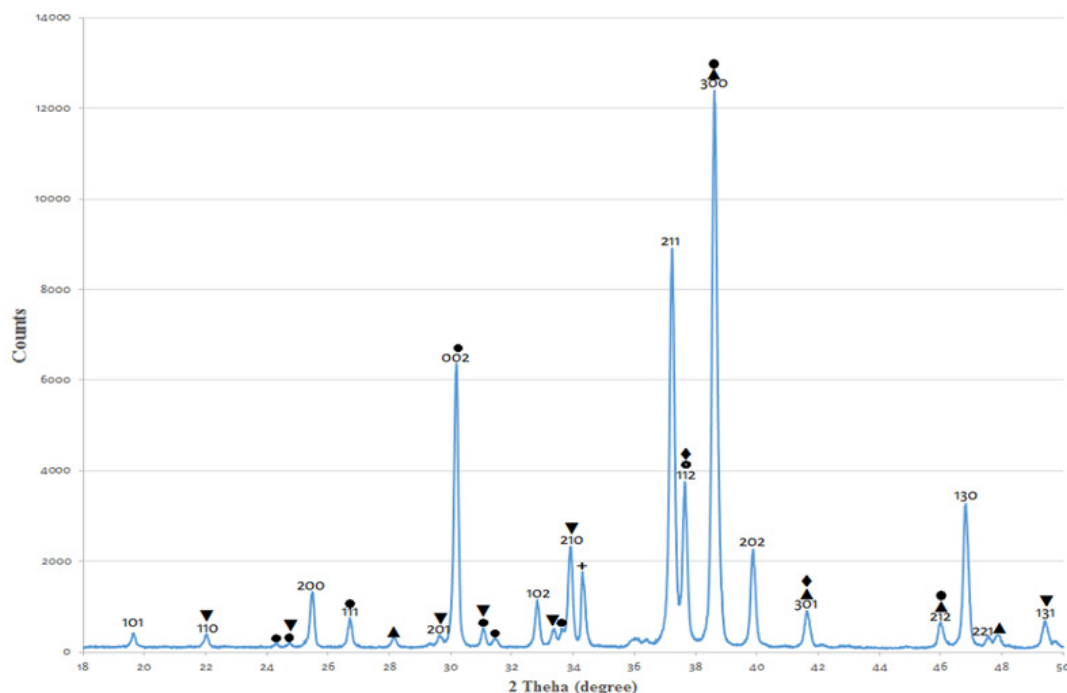


Figure 2: XRD pattern of initial phosphate concentrate. Miller indices of fluoroapatite are shown on the peaks. (Hematite ▲, Quartz ●, Monazite ▼, Maghemite ◆, Calcite +).

#### - Specific surface area and particle size distribution measurements

The BET surface area analyzer (Quantachrome Instruments CHEMBET-3000, USA) was used to measure changes in the specific surface area of phosphate concentrate due to mechanical activation. Particle size analyzer instrument (ANALY-

X-ray diffraction spectrum is the first step for extracting structural changes information. The present phases in the phosphate concentrate were identified by the Xpert High Score Plus software and the profile fitting was done by Winfit software. At first stage of profile fitting procedure, 10 peaks were selected with higher intensity and the initial

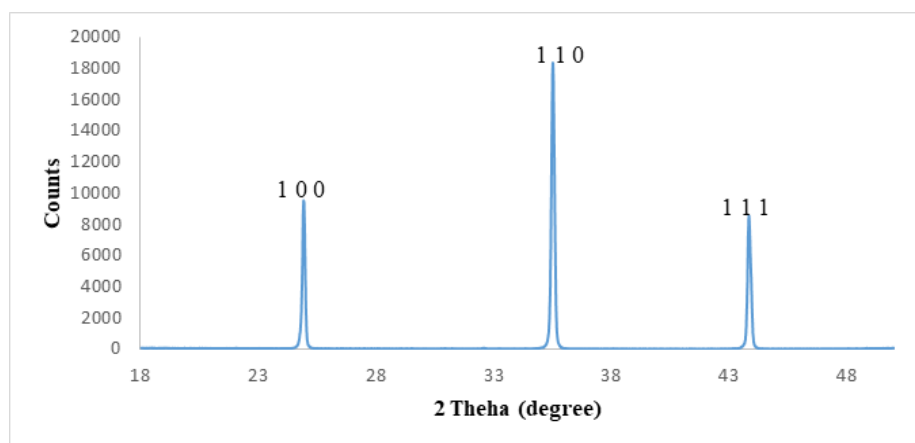


Figure 3: XRD pattern of standard LaB6 (SRM660a).

SETTE 22 Nano Tec plus, Fritsch, Germany) was used to measure particle size distribution, granulometric surface area, average particle size, and also to investigate the occurrence or absence of agglomeration phenomena during mechanical activation.

#### -XRD profile fitting procedure

The fitting of predetermined functions on the

information about micro-structure was introduced to the software. Assuming that the  $\kappa\alpha_2$  intensity is half of the  $\kappa\alpha_1$  intensity, the  $\kappa\alpha_2$  component was subtracted. Each x-ray diffraction profile was empirically fitted with a Pseudo Voigt function (Fig 4), a linear combination of the Lorentz or Gaussian function. After completion of fitting procedure, the instrumental broadening eliminated and the

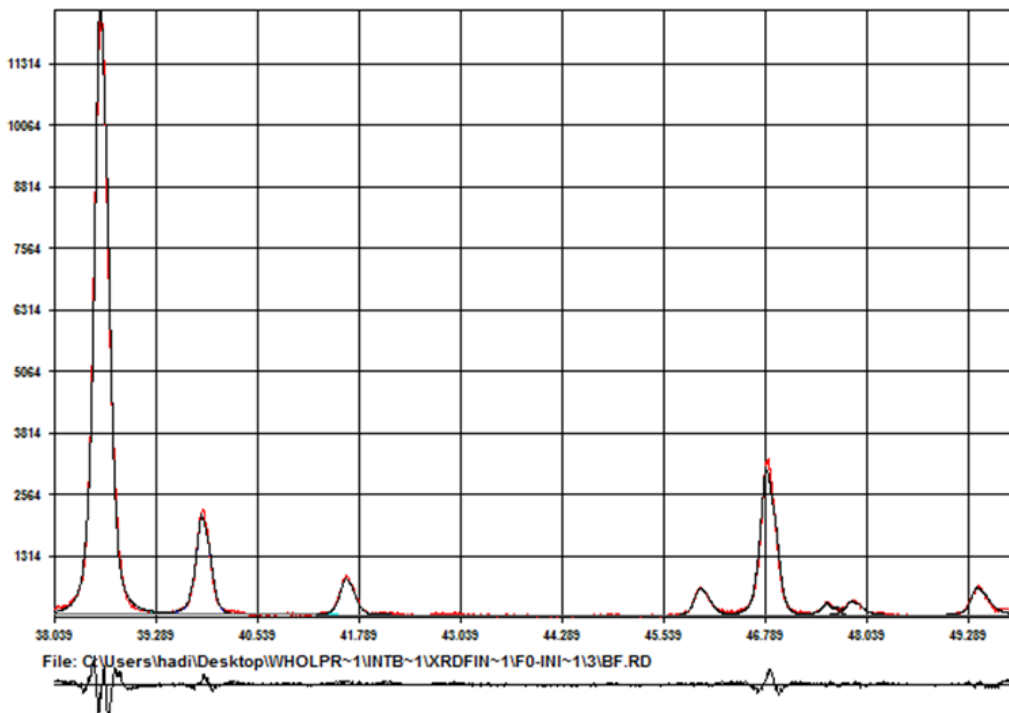


Fig 4: A typical profile fitting plot of initial phosphate concentrate conducted by Pseudo-Voigt function. The observed, measured patterns and their differences are pictured.

overlapped peaks were carefully separated [17]. Finally, the required initial data was obtained to calculate the micro-strain and crystallite size using the Williamson-Hall method and amorphization degree. The thirteen most intensive peaks of fluorapatite, such as (200), (111), (002), (102), (210), (211), (112), (300), (202), (301) (212), (130) and (131) were selected to measure structural changes.

#### Determination of degree of amorphization

The XRD peaks intensity represent the degree of disordering in the materials structure and by comparing them, it is possible to calculate the content of X-ray amorphous phase. The degree of amorphization is calculated using the following equation [18]:

$$A(\%) = 100 - (U_0/I_0 * I_x/U_x * 100) \quad (1)$$

In equation 1, U and I are attributed to the background and intensity of the XRD patterns, respectively. The zero index values represent the non-activated and the x index represents the mechanically activated XRD pattern.

#### Williamson- Hall integral breadth method

One of the good scales for determination of the mechanical activation intensity of various phases in the sample is using the Williamson-Hall integral breadth method. This method, invented in 1953, is one of the simplest and most widely used methods

for analyzing XRD patterns in order to simultaneously measure the crystallite size and the micro-strain. In the Williamson-Hall integral breadth method, broadening of peaks are associated with the combination of effective physical factors such as; the effect of the crystallites size and the micro-strain. In this method, the effectiveness of the mentioned factors after the deconvolution of the instrumental effects on the peaks broadening, by means of the relationships referred to below, are separated. If the XRD patterns are fitted with a combination of Gaussian and Lorentz functions, equation (5) is used to obtain physical broadening.

$$\beta_f = (\beta_h^2 - \beta_g^2) / \beta_h \quad (2)$$

$$B = (\beta_f \cos\theta) / \lambda \quad (3)$$

$$D = 2 \sin\theta / \lambda \quad (4)$$

$$B_2 = 1 / (D_v^2) + 4\varepsilon^2 D^2 \quad (5)$$

Where,  $\beta_f$  represents the measured (physical) integral breadth due to the effect of the crystallites size and the lattice-strain. Also,  $\beta_g$  and  $\beta_h$  represent instrumental and observed integral breadth, respectively; but  $\varepsilon$  is equal to lattice strain. Concepts such as total integral breadth and diffraction vector length are represented by B and D.

Plotting the  $B_2$  against  $D_2$ , gives a straight line with a slope equal to  $4\varepsilon^2$  and intercept of  $2D_v$ . It is obvious that in strain-free samples or samples



with very low micro-strain, the line slope in the Williamson-Hall plot will be close to zero and by increasing the micro-strain, the slope will increase.

### 3. Results and discussion

#### 3.1. Particle size surface area changes by milling

Table 3 shows how the mean particle size ( $d_{50}$ ), granulometric surface area (SG), BET surface area ( $S_{BET}$ ) and BET particle size ( $d_{BET}$ ) change with mechanical activation in planetary ball mill. Where  $d_{BET}$  is equal to diameter of equivalent particle with spherical shape, which is calculated from equation 6.

$$d_{BET} = 6 / (\rho S_{BET}) \quad (6)$$

$\rho$  is the density of apatite concentrate.

As shown in Table 3, the particle size has changed in two steps. At the first stage of mechanical activation,  $d_{50}$  of phosphate concentrate has a significant alteration. The maximum value of changes was related to samples which mechanically activated for 20 minutes with a ball to powder ratio of 20:1 and balls' diameter of 9.8 mm, so that the

tion was higher in the first 20 minutes and then changed with a lower slope. The highest variation was observed for the activated sample with a ball to powder ratio of 20:1 and 9.8 mm balls for 20 minutes, which was changed from 4.04  $m^2/g$  for phosphate concentrate (without activation) to 6.63  $m^2/g$  for activated sample. Previous studies have shown that with increasing mechanical activation time, the granulometric surface area decreased, but the BET specific surface increased, which is in good agreement with the above results [19, 20].

Table 3 expresses that granulometric surface area initially increased drastically and then decreased with a slight slope that is different from the BET surface area variation. Also, BET surface area is several times larger than granulometric surface area. High changes in granulometric and BET surface area indicate aggregation due to increased surface free energy, and the highest rate of changes was for mechanical activation by balls with larger surface area. If the particles adherence was tight and the nitrogen gas permeability (BET surface area) was decreased, an agglomeration process would have occurred that was not observed in the results tabulated in Table 3. Agglomeration and aggregation of mechanically activated particles have also been shown by previous investigators

Table 3: Specific surface area and particle size measurements of initial and mechanically activated phosphate concentrate by BET and laser diffraction analysis.

Activation time (min)	0	20	60	90	20	60	90	20	60	90
Ball to Powder ratio	-	20	20	20	20	20	20	40	40	40
Balls diameter (mm)	-	9.4	9.4	9.4	20	20	20	20	20	20
Rotation speed (rpm)	-	500	500	500	500	500	500	200	200	200
Granulometric surface area ( $m^2/gr$ )	1.14	2.61	1.93	1.81	1.94	2.09	1.84	2.07	1.99	1.95
mean particle size (D50) (microns)	16.3	4.6	7.1	7.6	9.6	9.2	10.5	8.3	8.1	7.3
BET surface area ( $m^2/gr$ )	4.04	6.63	6.81	6.9	6.44	6.72	6.84	5.81	5.93	6.11
BET mean particle size (microns)	0.48	0.29	0.284	0.28	0.30	0.29	0.28	0.34	0.33	0.32

particles size decreased from 16.3 microns for the initial sample to 4.6 microns for the mechanically activated sample. The results indicated that grinding rate in the first stage was severe and then, with increasing mechanical activation time, its rate decreased continuously. The results are in good agreement with previous researches [19].

In general, the BET surface area of phosphate concentrate has been increased because of mechanical activation, but, the slope of its varia-

[18-22].

The mechanical activation for 20 minutes reduced the of particles size of the phosphate concentrate significantly. By increasing the mechanical activation time from 20 to 60 and 90 minutes, the particles size has increased, which is more sensible in activation with smaller balls (Figure 1.A). The  $d_{80}$  of initial phosphate concentrate particles were 32.4 microns which have changed to 14, 19.6 and 20.5 microns after 20, 60 and 90 minutes of me-

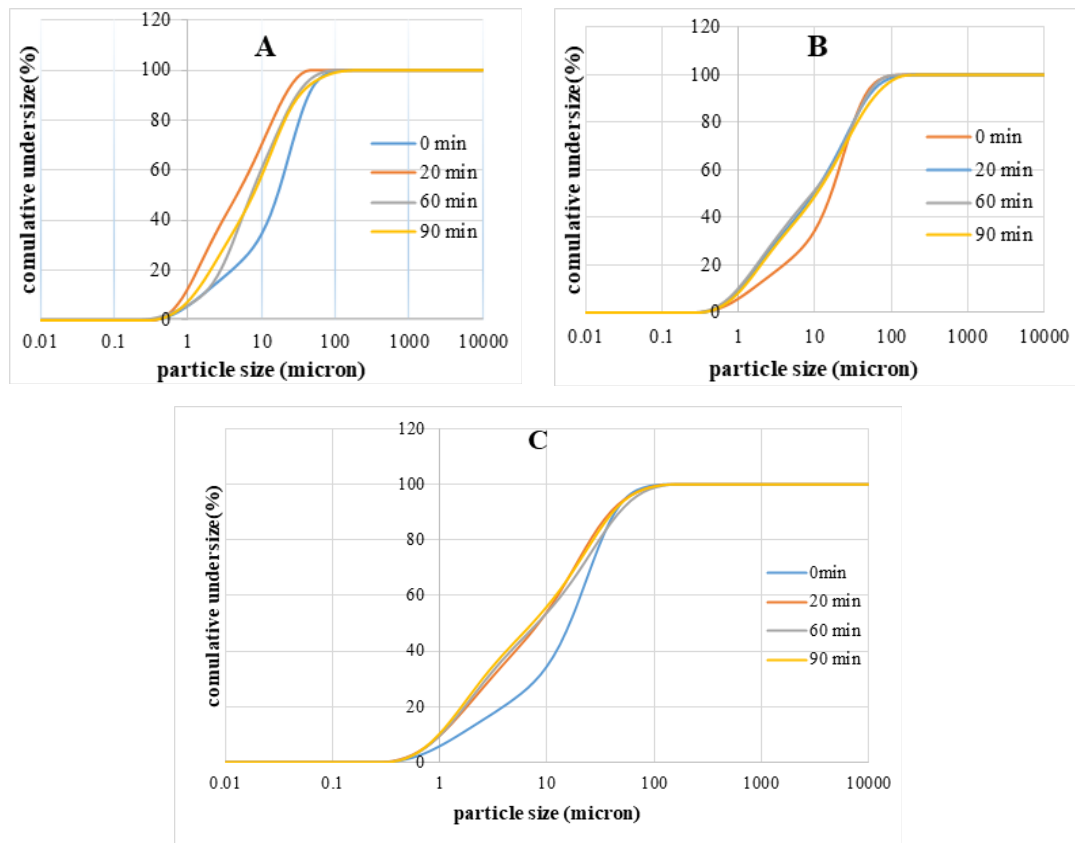


Figure 5: Cumulative undersize distribution curve of initial and activated phosphate concentrate by dry milling and argon atmosphere, A) Ball to powder ratio of 20:1, Balls diameter of 9.4 mm and rotation speed of 500 rpm. B) Ball to powder ratio of 20:1, Balls diameter of 20 mm and rotation speed of 500 rpm. C) Ball to powder ratio of 40:1, Balls diameter of 20 mm and rotation speed of 200 rpm.

chanical activation with small balls (Figure 1.A).

According to Figure 6, the predominant particle size in the primary phosphate concentrate is of a coarse grains type, and particles are present in a limited dimensional range. The mechanical activation for 20 minutes caused the particles to be ground and the coarse particles gradually replaced with fine particles, so that two types of particles with a small and coarse size are generated in the particle size distributing diagram, indicating that the grinding mechanism is abrasive. With the continuation of mechanical activation from 20 to 90 minutes, it is clearly seen that all the particles are

almost uniform, but the slope of the changes has decreased. The particle size distributing diagram moved toward the coarser particles and the particles became larger in size, indicating the accumulation of activated particles.

Unlike Figures 5.A and 7, which designate that mechanical activation with small balls causes a large changes in the particles size, there were no significant changes in the particles size of the activated samples with a ball to powder ratio of 40:1 (Figs 5C and 9). The main reason for the activated samples surface area to remain constant despite their increasing size, seems to be that the crushing

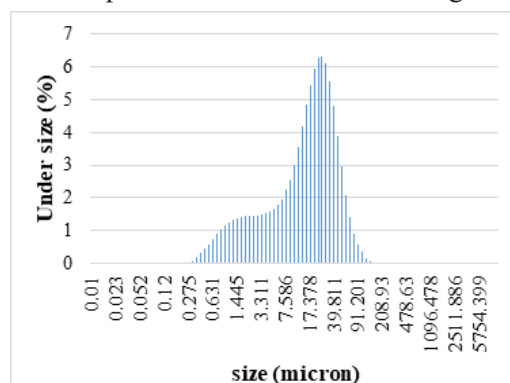


Figure 6: Initial phosphate concentrate particle size distribution diagram.

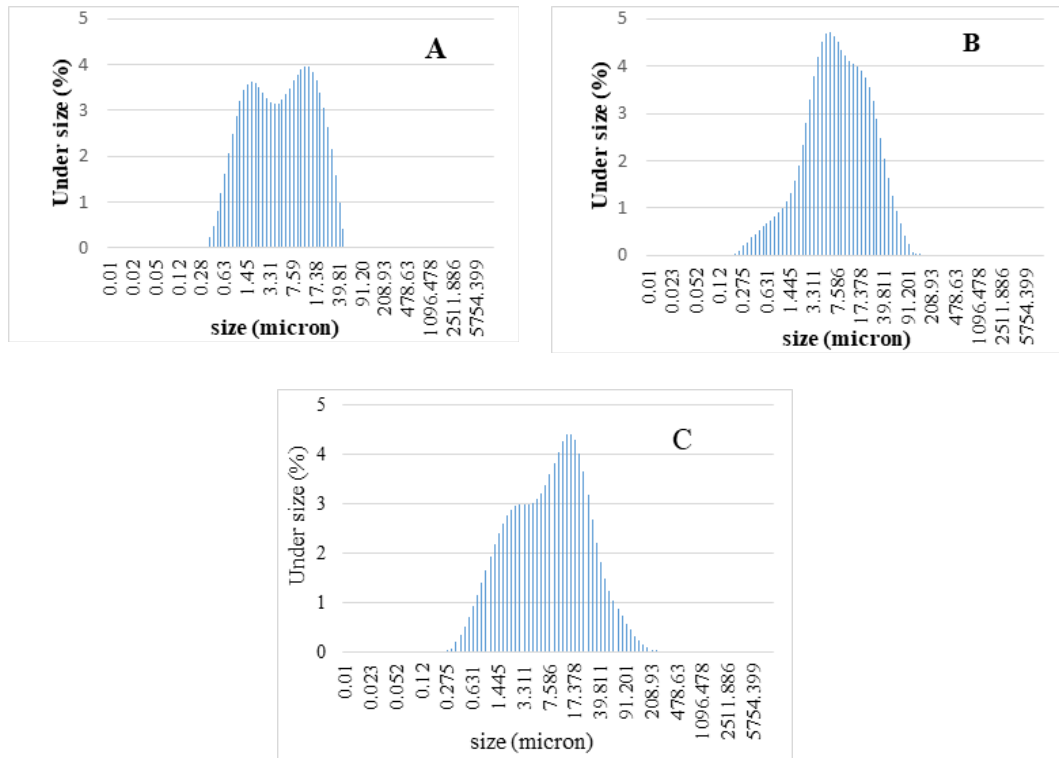


Figure 7: Particle size distribution diagram of mechanically activated phosphate concentrate at Ball to powder ration of 20:1, dry milling, argon atmosphere, balls diameter of 9.4 mm, rotation speed of 500 rpm and activation time of; A) 20 min, B) 60 min, C) 90 min

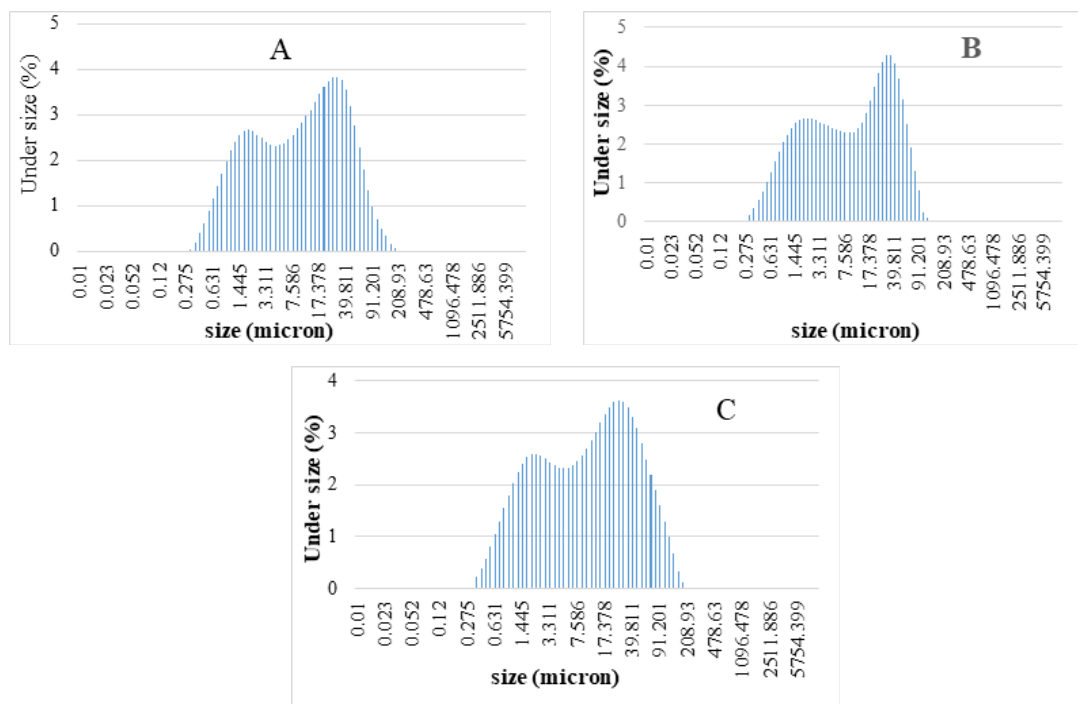


Figure 8: Particle size distribution diagram of mechanically activated phosphate concentrate at Ball to powder ration of 20:1, dry milling, argon atmosphere, balls diameter of 20 mm, rotation speed of 500 rpm and activation time of; A) 20 min, B) 60 min, C) 90 min.



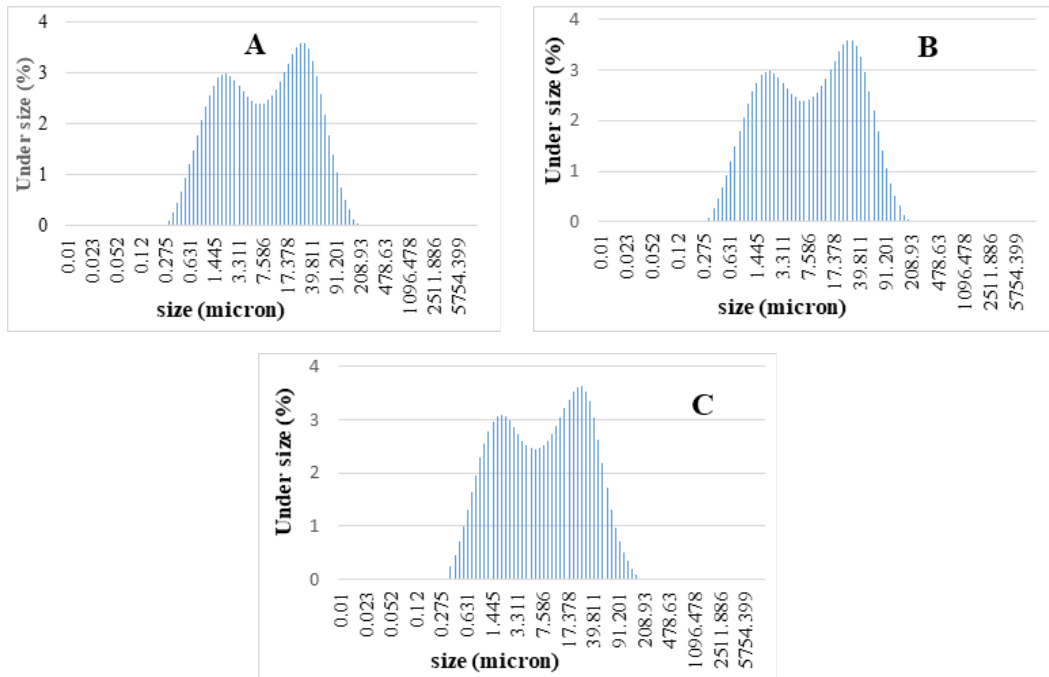


Figure 9: Particle size distribution diagram of mechanically activated phosphate concentrate at Ball to powder ratio of 40:1, dry milling, argon atmosphere, balls diameter of 20 mm, rotation speed of 200 rpm and activation time of; A) 20 min, B) 60 min, C) 90 min.

rate of the particles was equal to their aggregation rate.

In the particle size distribution diagram of initial phosphate concentrate, there is only one maximum point representing the distribution of particles in a limited dimensional range. In the particle size distribution diagrams of mechanically activated samples, two maximum points are seen. The maximum point in the small sizes is related to the ground par-

ticles, but the second point, which is larger in size, relates to the particles that are agglomerated.

### 3.2. Microstructure characterization using X-ray diffraction analysis

X-ray diffraction Patterns of the initial and mechanically activated phosphate concentrate are shown in Figure 10. No specific phase change has occurred due to mechanical activation. By increasing mechanical activation time, the breadth of the

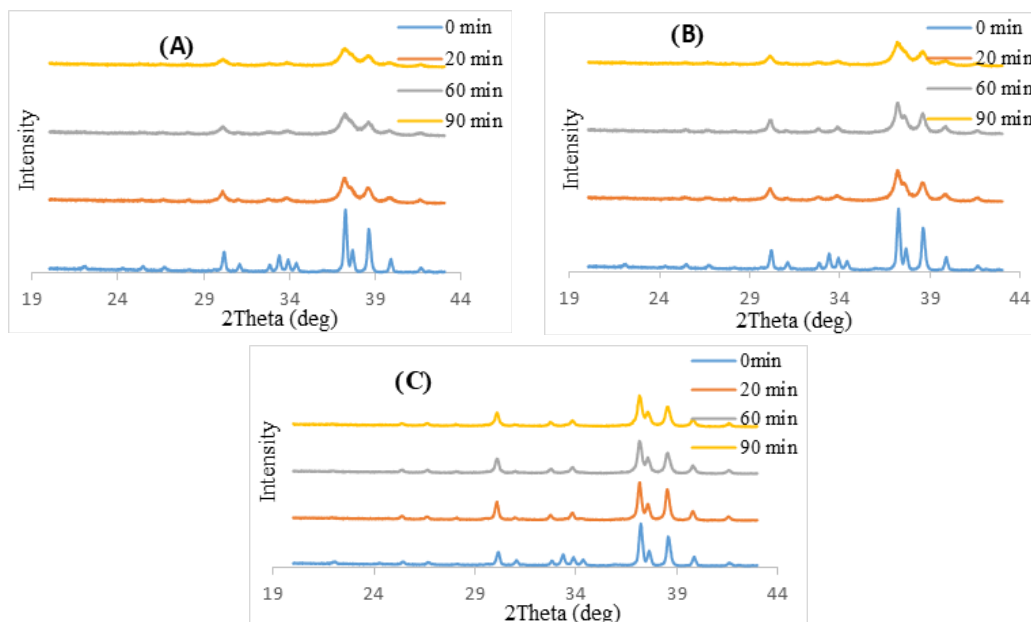


Figure 10: XRD analysis of initial and mechanically activated phosphate concentrate in the argon atmosphere and dry milling, A) ball/powder ratio of 20:1, 9.4 mm balls, rotation speed of 500 rpm, B) ball/powder ratio of 20:1, 20 mm balls, rotation speed of 500 rpm, C) ball/powder ratio of 40:1, 20 mm balls, rotation speed of 200 rpm.

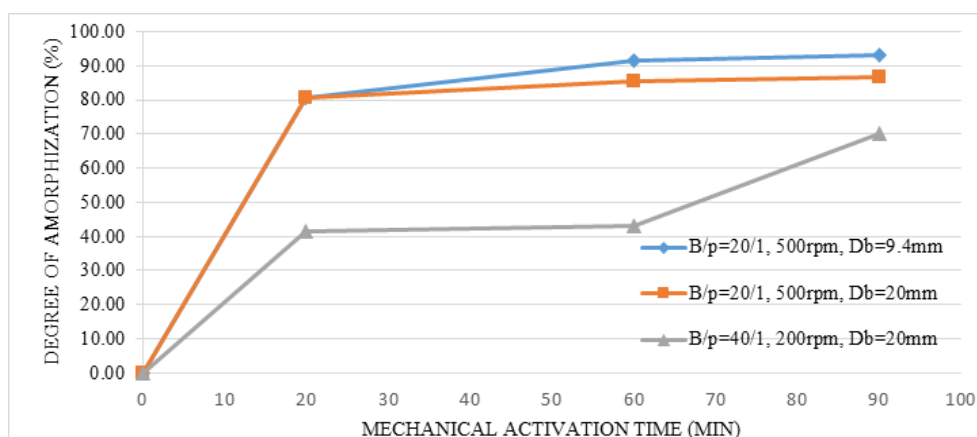


Figure 11: The variations in the degree of amorphization relative to the mechanical activation intensity (ball to powder ratio (B / P), rotation speed (rpm) and ball diameter (Db)) in the argon atmosphere and dry milling.

peaks has steadily increased and their height has decreased. X-ray diffraction changes showed that the crystalline structure of fluorapatite (the main phase of phosphate concentrate) has undergone fundamental changes. In order to quantitatively investigate these changes, the Williamson-Hall integral breadth method was used and the results are presented below.

According to the geometry of the diffracted peaks, the degree of x-ray diffraction amorphization (A) calculated using equation (1) (Figure 11). As x-ray diffraction analysis governs, The degree of amorphization increased sharply in the first stage of mechanical activation and its highest variation was related to mechanical activation with small balls (the highest specific surface area), reaching 93.38%, after 90 minutes of mechanical

activation. The relatively high degree of amorphization of mechanically activated samples, even in moderate milling conditions, indicates the non-refractory nature of phosphate concentrate during the mechanical activation. The least amount of amorphization is related to mechanical activation by balls with a lower specific surface area and a speed of 200 rpm, so that the effect of the milling rotation slowdown is higher than the increase in the ball to the powder ratio.

### 3.2.1. the crystallite size and micro-strain estimation using Williamson-Hall integral breadth method

Figure 12 shows the Williamson-Hall plots of the initial and mechanically activated phosphate concentrate. According to Equation 5, Williamson-Hall diagrams are plotted using linear regres-

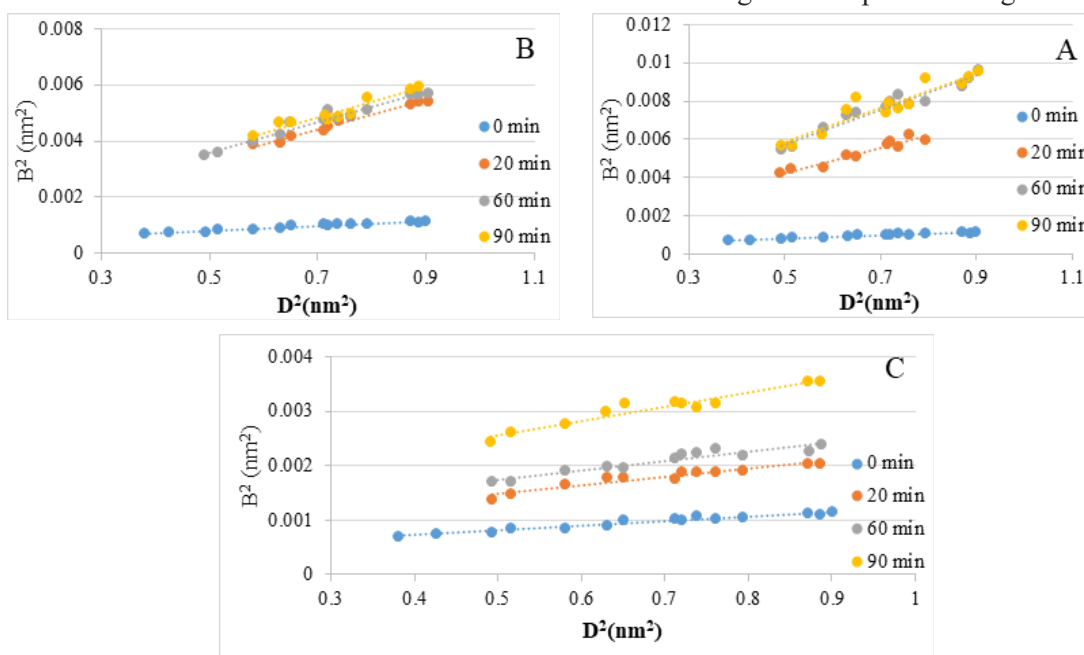


Figure 12: Williamson-Hall plots of the initial and mechanically activated phosphate concentrate in the Argon atmosphere and dry milling, A) ball/powder ratio of 20:1, 9.4 mm balls, rotation speed of 500 rpm, B) ball/powder ratio of 20:1, 20 mm balls, rotation speed of 500 rpm, C) ball/powder ratio of 40:1, 20 mm balls, rotation speed of 200 rpm.



Table 4. The summarized result of micro-strain and crystallite size measurements of initial and mechanically activated fluorapatite samples using Williamson-Hall integral breadth method.

Ball diameter (mm)	Rotation speed (rpm)	Milling time (min)	Crystallite size (nm)	Micro-strain (%)
-	-	0	225	0.09
9.4	500	20	90	0.66
9.4	500	60	69.23	0.89
9.4	500	90	64.29	0.9
20	500	20	112.5	0.51
20	500	60	100	0.53
20	500	90	90	0.55
20	200	20	128.5	0.15
20	200	60	100	0.17
20	200	90	69.2	0.26

sion method for the 10 main peaks of X-ray diffraction profile of fluorapatite. In the Williamson-Hall plots, none of the regression points was straight lines. This indicates that due to the hexagonal crystalline structure of fluorapatite, the crystallite size in different directions has a slight deviation. The results are in good agreement with previous research results [14-19]. The values of the crystallite size and micro-strain calculated from the linear regression are shown in Table 4.

Evidently, by increasing the mechanical activation time, the crystallite size is reduced and the micro-strain is increased. The slope of the changes in the first 20 minutes of mechanical activation was rapid but, with increasing the activation time, the slope of the changes was reduced. Due to the anisotropy in the XRD profiles, the crystallite size in different directions of reflection shows a slight difference. The Williamson-Hall method measures the mean values of all reflections in the entire XRD profile for micro-structure analyzing.

### 3.3.2. Lattice parameter and unit cell volume

Changes in the network parameter were calculated using UnitCell software. Table 5 shows the calculated values for cell parameters. Changes in the length of a, c and the unit cell volume were initially high and then were reduced with increasing mechanical activation time. The results revealed that with increasing mechanical activation time, the parameter of fluorapatite cell increased and the unit cell volume increased as well, therefore, it can be concluded that mechanical activation has led to the expansion of unit cell. The data related to the cell parameter and unit cell volume with 95% confidence level have been calculated. According to Figures 13 and 14, as well as the results of variations in the crystallite size and micro-strain, the greatest amount of variation was related to mechanical activation with smaller steel balls. Therefore, it can be seen that with increasing the level of the balls, the microstructure of fluorapatite changes has increased. So, it can be concluded that by increasing the specific surface area of the balls, the

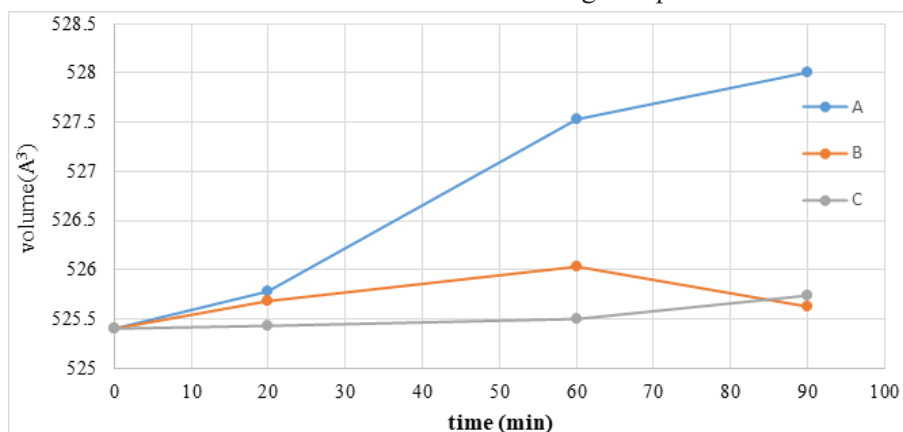


Figure 13: unit cell volume changes as a function of mechanical activation time, A) ball/powder ratio of 20:1, 9.4 mm balls and rotation speed of 500 rpm, B) ball/powder ratio of 20:1, 20 mm balls and rotation speed of 500 rpm, C) ball/powder ratio of 40:1, 20 mm balls and rotation speed of 200 rpm.

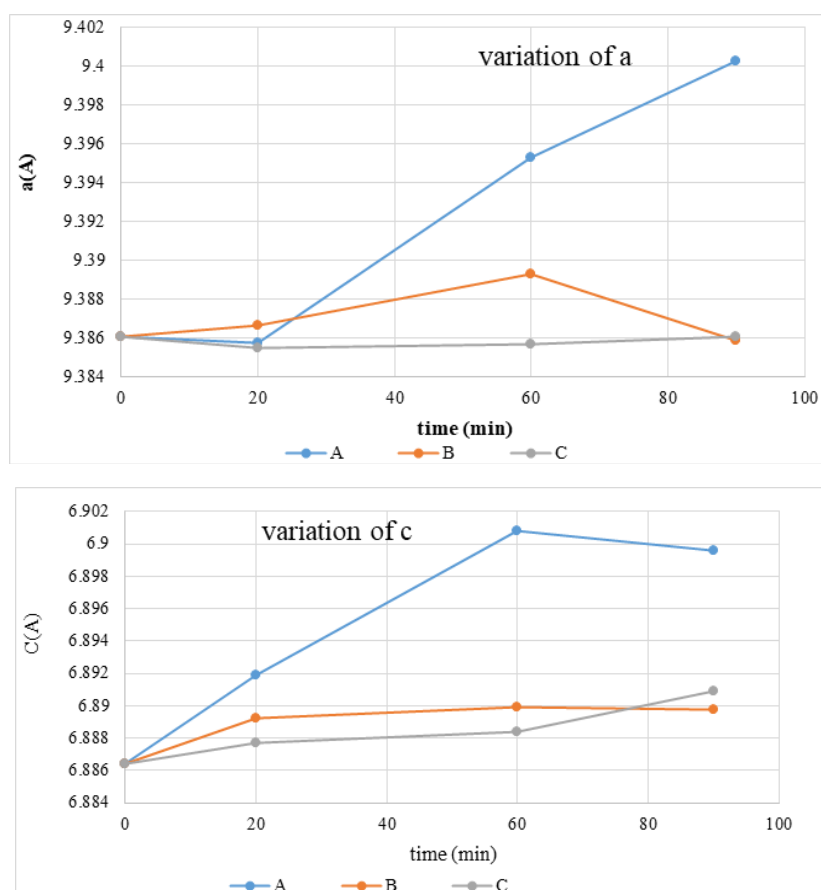


Figure 14: cell parameters variation in two direction of a and c as a function of mechanical activation time A) ball/powder ratio of 20:1, 9.4 mm balls and rotation speed of 500 rpm, B) ball/powder ratio of 20:1, 20 mm balls and rotation speed of 500 rpm, C) ball/powder ratio of 40:1, 20 mm balls and rotation speed of 200 rpm.

microstructure changes of fluorapatite increased.

According to the results of Figures 13 and 14, the changes in the cell parameter in the c direction have a greater effect than a direction, on the volume changes of the unit cell. In some cases, in spite of reducing of a cell parameter, the unit cell volume increased with the increase of the c cell parameter.

#### 4. Conclusions

Different conditions of ball milling was used in this study to understand the induction of structural changes during mechanical activation of phosphate concentrate. It was concluded that using of higher balls surface area and longer times of mechanical activation, higher surface area, amorphization degree, micro-strain, dislocation and broadened integral XRD lines are achieved; but crystallite size and intensity of XRD peaks of activated powder decreased. The results showed that mechanical activation can change crystallite size and micro-strain from 225 nm and 0.09 % (initial sample) to 64.24 nm and 0.9 % after 90 min of high energy milling, respectively.

The specific surface area measurements showed that, increasing of activation time can cause to increase of activated sample's surface area and agglomeration of them. The size distribution curves showed two maximum point that the first point is related to fine particles and the second one is related to the agglomerated particles. Comparing of granulometric and BET surface area indicated that in initial stages of agglomeration, the particle pores were available for nitrogen gas penetration but with increasing of activation time, the agglomeration was more intense and the pores between the particles were closed.

The unit cell volume changes indicated that mechanical activation can increase fluorapatite cell volume and the increasing of the mechanical activation intensity intensifies cell volume changes. The alterations in the cell parameter in the c direction have a greater effect on the volume changes of the unit cell than a direction. In some cases, in spite of reducing of a cell parameter, the unit cell volume increased with the increase of the c cell parameter.



## References

1. Juhász, A.Z., 1998. Aspects of mechanochemical activation in terms of comminution theory. *Colloids and Surfaces A: Physicochemical and Engineering Aspects*, 141(3), pp.449-462.
2. Pourghahramani, P. and Forssberg, E., 2006. Microstructure characterization of mechanically activated hematite using XRD line broadening. *International Journal of Mineral Processing*, 79(2), pp.106-119
3. Baláž, P., 2000. *Extractive metallurgy of activated minerals* (Vol. 10). Elsevier.
4. Tkáčová, K., 1989. Mechanical activation of minerals. *Veda*.
5. Boldyrev, V.V., Pavlov, S.V. and Goldberg, E.L., 1996. Interrelation between fine grinding and mechanical activation. In *Comminution 1994* (pp. 181-185).
6. Karagedov, G. and Lyakhov, N., 2003. Mechanochemical grinding of inorganic oxides. *KONA Powder and Particle Journal*, 21, pp.76-87.
7. Pourghahramani, P. and Forssberg, E., 2006. Comparative study of microstructural characteristics and stored energy of mechanically activated hematite in different grinding environments. *International Journal of Mineral Processing*, 79(2), pp.120-139.
8. Yang, F.Q. and Chao, W.U., 2013. Mechanism of mechanical activation for spontaneous combustion of sulfide minerals. *Transactions of Nonferrous Metals Society of China*, 23(1), pp.276-282.
9. Li, J. and Hitch, M., 2017. Ultra-fine grinding and mechanical activation of mine waste rock using a planetary mill for mineral carbonation. *International Journal of Mineral Processing*, 158, pp.18-26.
10. Borouni, M., Niroumand, B. and Maleki, A., 2018. A study on crystallization of amorphous nano silica particles by mechanical activation at the presence of pure aluminum. *Journal of Solid State Chemistry*, 263, pp.208-215.
11. Mejdoub, R., Hammi, H., Khitouni, M., Suñol, J.J. and M'nif, A., 2017. The effect of prolonged mechanical activation duration on the reactivity of Portland cement: Effect of particle size and crystallinity changes. *Construction and Building Materials*, 152, pp.1041-1050.
12. Baláž, P., Turianicová, E., Fabián, M., Kleiv, R.A., Briančin, J. and Obut, A., 2008. Structural changes in olivine (Mg, Fe)  $2\text{SiO}_4$  mechanically activated in high-energy mills. *International Journal of Mineral Processing*, 88(1-2), pp.1-6.
13. Li, J. and Hitch, M., 2016. Characterization of the microstructure of mechanically-activated olivine using X-ray diffraction pattern analysis. *Minerals Engineering*, 86, pp.24-33.
14. Pourghahramani, P. and Forssberg, E., 2007. Changes in the structure of hematite by extended dry grinding in relation to imposed stress energy. *Powder Technology*, 178(1), pp.30-39.
15. Pourghahramani, Parviz, and Eric Forssberg. "Comparative study of microstructural characteristics and stored energy of mechanically activated hematite in different grinding environments." *International Journal of Mineral Processing* 79.2 (2006): 120-139.
16. Pourghahramani, Parviz. "Mechanical Activation of hematite using different grinding methods with special focus on structural changes and reactivity." PhD diss., Luleå tekniska universitet, 2007.
17. Halder, N.C. and Wagner, C.N.J., 1966. Separation of particle size and lattice strain in integral breadth measurements. *Acta Crystallographica*, 20(2), pp.312-313.
18. Baláž, P., Mechanical activation in hydrometallurgy. *International Journal of Mineral Processing*, 2003. 72(1): p. 341-354..
19. Pourghahramani, P. and Akhgar, B.N., 2015. Characterization of structural changes of mechanically activated natural pyrite using XRD line profile analysis. *International Journal of Mineral Processing*, 134, pp.23-28.
20. Atashin, Sanam, John Z. Wen, and Robert A. Varin. "Investigation of milling energy input on structural variations of processed olivine powders for CO<sub>2</sub> sequestration." *Journal of Alloys and Compounds* 618 (2015): 555-561.
21. Bohács, K., Kristály, F. and Mucsi, G., 2018. The influence of mechanical activation on the nanostructure of zeolite. *Journal of Materials Science*, 53(19), pp.13779-13789.